Hyperbranched Rigid Aromatic Phosphorus-Containing Flame Retardants for Epoxy Resins

Alexander Battig, Patrick Müller, Annabelle Bertin, and Bernhard Schartel*

A rigid aromatic phosphorus-containing hyperbranched flame retardant structure is synthesized from 10-(2,5-dihydroxyphenyl)-10H-9-oxa-10-phosphaphenanthrene-10-oxide (DOPO-HQ), tris(4-hydroxyphenyl) phosphine oxide (THPPO), and 1,4-terephthaloyl chloride (TPC). The resulting poly-(DOPO-HQ/THPPO-terephthalate) (PDTT) is implemented as a flame retardant into an epoxy resin (EP) at a 10 wt% loading. The effects on EP are compared with those of the monomer DOPO-HQ and triphenylphosphine oxide (OPPh$_3$) as low molar mass flame retardants. The glass transition temperature, thermal decomposition, flammability (reaction to small flame), and burning behavior of the thermosets are investigated using differential scanning calorimetry, thermogravimetric analysis, pyrolysis combustion flow calorimetry, UL 94-burning chamber testing, and cone calorimeter measurements. Although P-contents are low at only 0.6 wt%, the study aims not at attaining V-0, but at presenting a proof of principle: Epoxy resins with PDTT show promising fire performance, exhibiting a 25% reduction in total heat evolved (THE), a 30% reduction in peak heat release rate (PHRR) due to flame inhibition (21% reduction in effective heat of combustion (EHC)), and an increase in T_g at the same time. This study indicates that rigid aromatic hyperbranched polymeric structures offer a promising route toward multifunctional flame retardancy.

1. Introduction

The release of flame retardants into the environment has long been identified to be problematic,[1] particularly the tendencies of low molecular weight flame retardants to leach or bloom out during the lifetime of consumer products. The use of halogenated flame retardants has been under discussion for several decades. Several substances of this class have been banned, and growing market demands have prompted the development of halogen-free alternatives. For the last decade, REACH (Registration, Evaluation, Authorization and Restriction of Chemicals) has been addressing the development of less persistent, bioaccumulating, and toxic materials in the European Union. Notably, polymeric flame retardants, especially those containing phosphorus, are promising contenders for this category.[2] It is not surprising that the development of flame retardants with complex oligomeric or polymeric structures is a trend in the branch of halogen-free markets.[3–10] Polymerization reduces the undesired leaching or release of volatile low molar mass flame retardants by integrating them into a macromolecular structure inside a polymer matrix, thereby minimizing negative effects on glass-transition temperature (T_g) and mechanical properties of the material. Moreover, the flame retardants' solubility in water is essentially diminished, thereby lowering the threat of potential bioaccumulation or toxicity.

Subgroups of oligomeric or polymeric flame retardants are molecules with complex geometries and hyperbranched polymers, respectively. They have a multifaceted geometry, possess a large number of reactive or functional groups, acceptable miscibility with polymers, ease of processability, and usually exhibit low crystallinity.[11–14] Hyperbranched polymers can be easily produced in a one-pot synthesis, as their polymeric structure is achievable in a single reaction step, making them ideal for preparation on a large scale.[15,16] Compared to conventional flame retardant additives, those with hyperbranched and complex structures harbor the potential to show reduced negative effects on other polymer properties such as material properties or T_g, which is highly desirable, but rare for flame retardants. Recent publications have highlighted the use of hyperbranched polymers as flame retardants.[17] Moreover, hyperbranched polymers based on phosphorus often present multifunctional qualities, for example, improving the mechanical properties as toughening agents or increasing T_g.[18–20] The flame retardant modes of action and chemical decomposition mechanisms of a series of phosphorus-based hyperbranched polymers has been examined in detail, highlighting the multifunctional qualities of these flame retardant additives.[7,21–26]

Dr. A. Battig, Dr. P. Müller, Dr. A. Bertin, Prof. B. Schartel
Bundesanstalt für Materialforschung und –prüfung (BAM)
Unter den Eichen 87, Berlin 12205, Germany
E-mail: bernhard.schartel@bam.de
Dr. A. Bertin
Institute of Chemistry and Biochemistry
Freie Universität Berlin
Takustr. 3, Berlin 14195, Germany

ADVANCED
SCIENCE NEWS
www.advancedsciencenews.com

Macromolecular
Materials and Engineering
www.mme-journal.de

Previous investigations into the chemical structure of hyper-branched polymers have yielded a road-map to synthesizing effective hyperbranched polymeric flame retardants: the oxidation state of phosphorus plays a role in the flame retardant chemical mechanisms and mode of actions,[27] as does the chemical surrounding of phosphorus.[28] Moreover, an aromatic backbone has been proven effective in lowering heat evolution, lowering smoke production, and decreasing combustion efficiencies.[25] One hitherto uninvestigated route involves the synthesis of a rigid hyperbranched structure using a planar branching point and stiff, rod-like branches, which this study aims to investigate as an effective flame retardant structure with superior properties.

This paper presents the results of a study aimed at assessing the flame retardancy effect of a halogen-free, phosphorus-containing hyperbranched aromatic flame retardant with a rigid structure in an epoxy resin, specifically in diglycidyl ether of bisphenol A (DGEBA) cured with isophorone diamine (IPDA). The polymeric flame retardant is based on three parts: a) a derivate of 9,10-dihydro-9-oxa-10-phosphaphenanthrene-10-oxide (DOPO) which was chemically bound to hydroquinone to form a bifunctional phenol 10-(2,5-dihydroxyphenyl)-10H-9-oxa-10-phosphaphenanthrene-10-oxide (DOPO-HQ); b) a trifunctional phenol based on tris(4-hydroxyphenyl)phosphine oxide (THPPO), which acted as a branching point; and c) a bifunctional acid chloride 1,4-terephthaloyl chloride (TPC). The resulting flame retardant, referred to as poly-(DOPO-HQ/THPPO-terephthalate) (PDTT), was generated via polycondensation. The chemical structure of the material is key, encompassing several moieties targeting not only enhanced fire performance, but additional benefits such as an increase in T_g. Previous investigations into aromatic hyperbranched polymers have shown that aromatic flame retardants exhibit an enhanced condensed phase mode of action via charring compared to aliphatic variants.[25] Moreover, the implementation of phosphine oxides and DOPO-moieties is aimed at enhancing a gas phase mode of action,[27,29] and as previous studies have shown, multicomponent flame retardant systems containing multiple phosphorus "types", that is, species of varying chemical surrounding, are beneficial to fire performance.[30] Furthermore, the presence of aromatic rings and bulky pendant DOPO-groups leads to a high molecular rigidity, with the objective of increasing T_g. Finally, the complex shape promotes miscibility with the polymer matrix, as previous studies into hyperbranched polymers[31,32] and polymers with rigid and complex geometries have shown.[33]

In the approach presented herein, the flame retardants were incorporated into an epoxy resin at a loading of 10 wt%. The flame behavior of the resulting blends were assessed and compared with similar blends containing low molar mass flame retardants. Two different low molar mass flame retardants were chosen, corresponding to the subunits of the proposed polymeric flame retardant, namely DOPO-HQ and triphenylphosphine oxide (OPPh$_3$), the latter similar to THPPO, the synthesis of which has been previously described.[34] The synthesis of DOPO-HQ has been described previously,[35] and it has been used in several synthesis routes as a flame retardant,[36,37] also for epoxy resins.[38–40] Specimens for reaction-to-small-flame tests and for the forced-flaming-combustion test were prepared,

and the flame retardancy performance was assessed for different fire scenarios. From the results, the modes of action in the gas phase and in the condensed phase have been proposed.

It was expected that the phosphorus-content of the material is insufficient, at the level loaded, to afford a V-0 classification for an epoxy matrix, yet the aim of this study is not the optimization of a commercial product, but rather to provide a proof of the underlying principle. Polymeric flame retardants with complex geometries have the potential to play a significant role in future flame retardant formulations, especially for phosphorus-based non-halogenated materials. The investigation of the effectiveness of this material, which is based on rigid and already successful phosphorus-based structures, expands upon the understanding of the function of hyperbranched flame retardants and provides valuable insight into the possibilities of synthetic chemistry, especially when aimed at producing macromolecules with complex geometries.

2. Results and Discussion

2.1. PDTT Synthesis and Characterization

The flame retardant PDTT shown in **Scheme 1** was synthesized by solution polycondensation of a bifunctional phenol, 10-(2,5-diihydroxyphenyl)-10H-9-oxa-10-phosphaphenanthrene-10-oxide (DOPO-HQ), and a trifunctional phenol tris(4-hydroxy-phenyl)phosphine oxide (THPPO) with a bifunctional acid chloride, namely 1,4-terephthaloyl chloride (TPC). THPPO was used to provide a branching point. The reaction was carried out at RT under inert atmosphere in anhydrous dichloromethane using triethylamine as a base and 4-N,N-dimethylaminopyridine (DMAP) as a catalyst. It should be mentioned that only terephthaloyl chloride was readily soluble in dichloromethane, but the other monomers were consumed during the gel formation.

Obviously, the presented synthesis route is merely a first approach which acts as a proof of principle that leaves plenty of room for optimization and improvement. The selected route is replaceable by synthesis routes that deliver controlled branching degrees and molecular weights. Future works may be improved by utilizing various approaches for A_2+B_3 type polymerizations[11,41] and also by addressing high conversions while avoiding gelation.[42]

2.2. Molecular Dynamic Modeling

While the structure of PDTT shown in Scheme 1 displays the chemical formula, spatial geometry considerations of the molecule provide greater insight into the advantageous properties. **Figure 1** displays a molecular dynamic simulation of several segments of the polymer. The structures were modeled using a force field type MM2 and were minimized to the lowest energetic state for each conformation until the RMS gradient was 0.01.

Although the molecular shapes of the phosphine oxide units in THPPO/ OPPh$_3$ are tetrahedral, that is in sp^3 hybridization, the shape resembles a flattened tripod, as three bonds connect from the central phosphorus atom to 4-hydroxyphenols and one
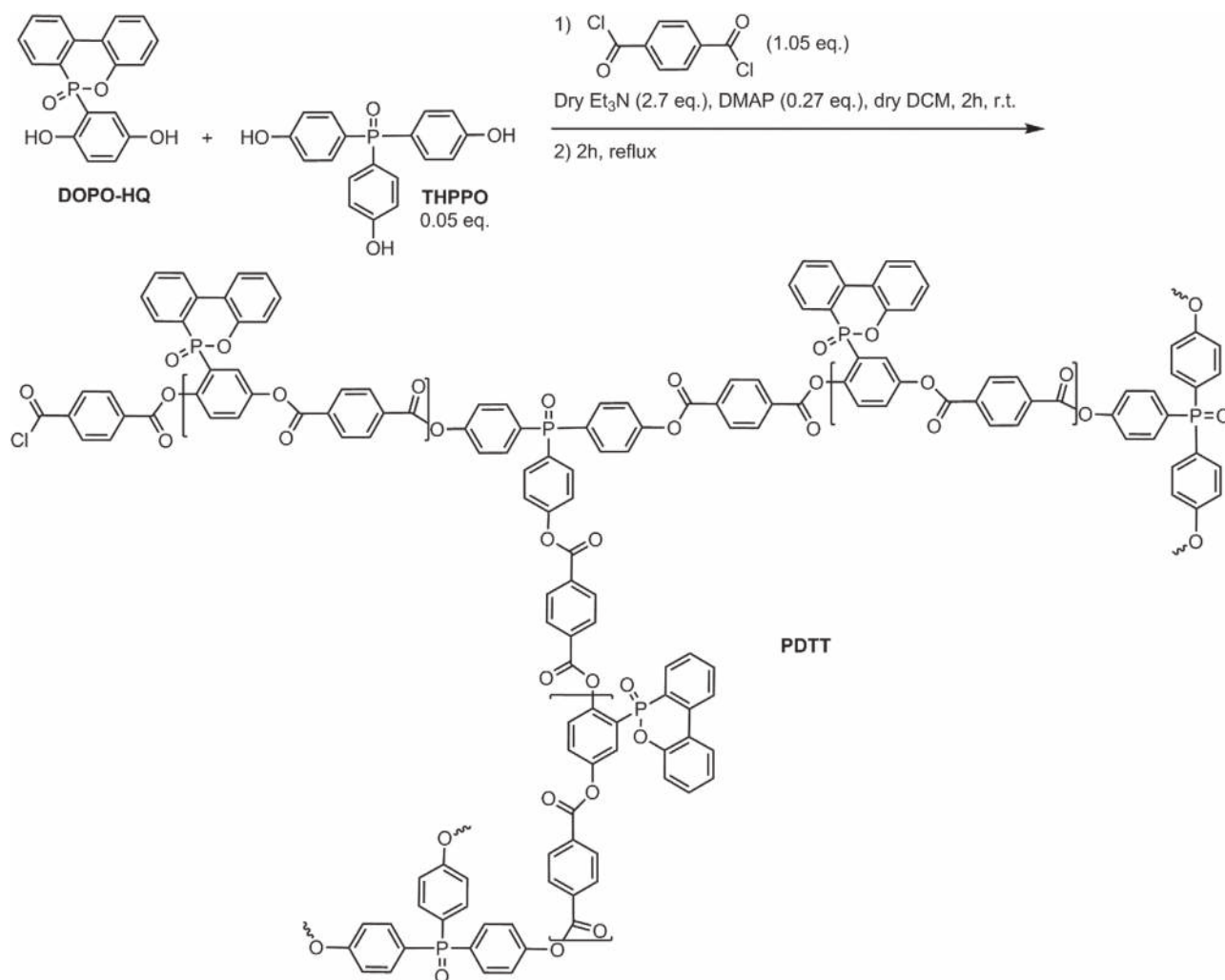
Scheme 1. Reaction scheme of PDTT synthesis via polycondensation reactions of DOPO-HQ and THPPO with TPC.

double bond connects to oxygen. Furthermore, the connecting aromatic rings, due to steric hinderances, are not in the same plane relative to one another, but connected at an angle to the central P atom (Figure 1a). Moving along the backbone, the connecting terephthalic ester groups lie at a torsional angle relative to the hydroquinone-units of DOPO-HQ (Figure 1b), as Lautenschläger et al. stipulated for aromatic esters.[43] As a result, the tetrahedron structure of the phosphine oxide is mitigated and the branching point becomes more planar (Figure 1c,d). When comparing triphenyl phosphine oxides to triphenyl phosphates, the phosphine oxide is more rigid, as the presence of P−O−C_{arom} bonds in phosphates have a different rotational flexibility than P−C_{arom} bonds.

Branching off the THPPO/ OPPh$_3$ units, the backbone of (DOPO-) hydroquinone–terephthalic ester moieties is freely rotational along its axis, yet the linear molecular structure itself is highly rigid. These structural considerations provide insight into the molecule's function: the complex architecture results from stiff, rod-like (DOPO-) hydroquinone–terephthalic ester "arms" extending from relatively planar tripod THPPO/ OPPh$_3$ branching units.

When examining the molecular model and shape of this flame retardant, it is unlikely that intramolecular cross-linking reactions occur during synthesis. Moreover, the flame retardant's improved miscibility is more closely understood, as the group of Wendorff investigated the impact of rigid multipode geometries on polymer matrix miscibility.[33,44]

2.3. Preparation of Flame-Retarded Epoxy Resin Samples

For each respective flame-retarded formulation, DGEBA and IPDA (ratio 100:25) and 10 wt% of the flame retardant were combined in a glass beaker and thoroughly mixed with a mechanical stirrer for at least 10 min. The mixture was poured into open aluminum molds with a layer height of 3 mm and placed into an oven for 30 min at 80 °C, 30 min at 110 °C, and 60 min for 160 °C. The samples were slowly cooled to RT to avoid cracking, and then cut down to plates sized 100 × 100 mm (for cone calorimeter measurements) or strips of 13 mm width (for UL 94 testing), respectively. Some material was also cryomilled to obtain powdered sample material.
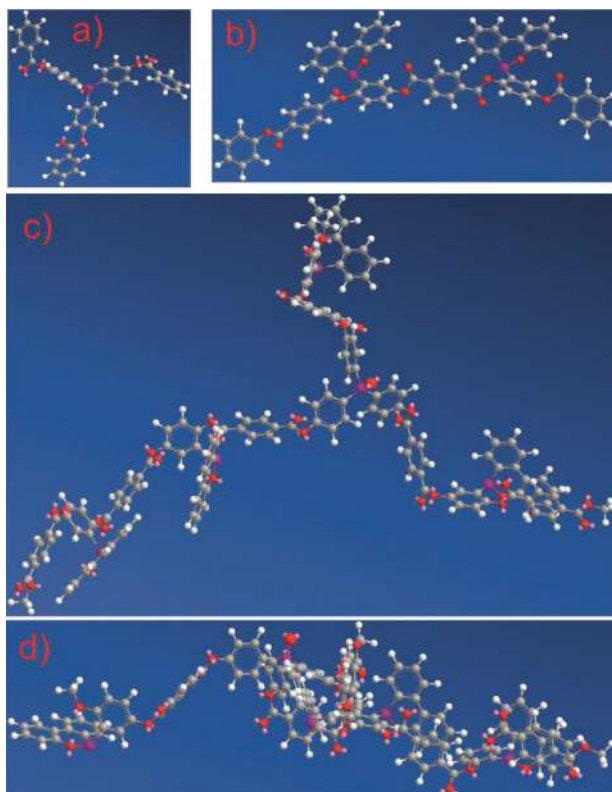
Figure 1. Molecular dynamic modeling of PDTT and subunits thereof; a) THPPO/ OPPh₃ units (branching points); b)(DOPO-)hydroquinone–terephthalic ester moieties; c) PDTT oligomer subunit (top down view); d) PDTT oligomer subunit (view in plane). Color code: Phosphorus = purple, carbon = grey, hydrogen = white, oxygen = red.

The primary alcohol groups in THPPO interfered with the crosslinking reaction of DGEBA and IPDA, in part due to the high reactivity of these hydroxyl groups. Therefore, OPPh₃ was used as a model system to simulate the function of THPPO in flame retarded epoxy resin mixtures.

OPPh₃ had a phosphorus content of approx. 11.1 wt%. For DOPO-HQ, the content was about 9.55 wt%, and PDTT had a calculated phosphorus content of 6.0 wt%. The loading of flame retardant in resin blends was 10 wt% in all cases, meaning that the resulting flame retarded polymer resins had effective phosphorus contents of 1.1 wt% (EP + OPPh₃), 1.0 wt% (EP + DOPO-HQ), and 0.6 wt% (EP + PDTT).

2.4. Glass-Transition Temperature

The T_g of the materials were investigated by differential scanning calorimetry (DSC) to identify the impact of the flame retardants on the material properties of the epoxy resin (EP). The corresponding results are shown in **Figure 2**.

The glass-transition temperature of DGEBA cured with IPDA usually spanned a range between 138 °C to 164 °C, depending on the methodology of the curing process. More carefully (i.e., slowly) cured samples usually attain higher T_gs. The herein prepared EP exhibited a T_g of 154 °C, which is very typical for well-prepared DGEBA-based resins.[45]
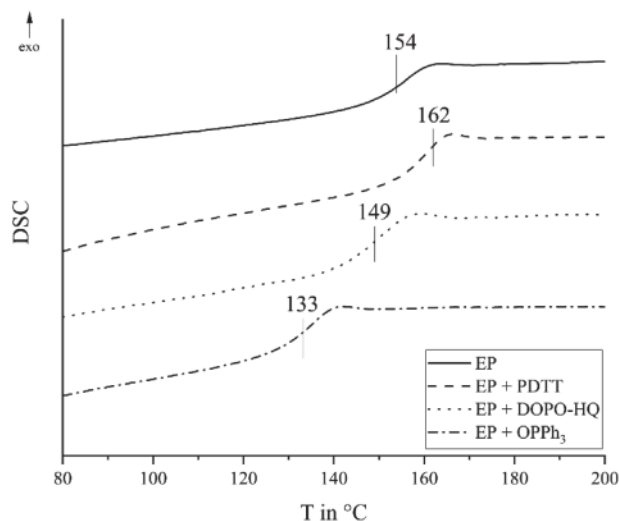
Figure 2. DSC curves of epoxy resins and marked T_gs; values have an error of ±2 °C.

The addition of flame retardants altered the glass transition temperatures of EP in different ways. DOPO-HQ lowered the T_g of EP moderately by 5 °C, while OPPh₃ lowered it by 21 °C. The crucial drop in glass-transition temperature for EP + OPPh₃ is explained by the plasticizing effect common to low molar mass additives with good solubility, especially those with spherical shapes.[32,46,47] For DOPO-HQ, the dilution of the network and thus the decrease in cross-linking density lowered the T_g, too. However, the bulky character of the rather stiff DOPO-HQ group yielded a smaller plasticizing effect than OPPh₃.

The glass-transition temperature of EP + PDTT was increased by 8 °C compared to EP, unlike DOPO-HQ and OPPh₃. This increase is due to the increased miscibility, rigid molecule structure, and high content of bulky aromatic groups present in the structure of PDTT, as shown in molecular dynamic modeling. Moreover, PDTT's complex shape acted as additional physical net-points between the epoxy resin structure and the macromolecular flame retardant, which overall elevated the T_g of EP + PDTT.

2.5. Thermal Decomposition

The thermal decomposition of PDTT, DOPO-HQ, OPPh₃, and THPPO, as well as EP, EP + PDTT, EP + DOPO-HQ, and EP + OPPh₃ was investigated via thermogravimetric analysis (TGA). The results are shown in **Table 1** and **Figure 3**.

PDTT exhibited three decomposition steps with a residue yield of 43.9 wt% at 900 °C, the highest of all tested flame retardants (Figure 3a). The decomposition steps correspond to the cleavage of the DOPO and THPPO/ OPPh₃ moieties, respectively, as made evident by the thermal decomposition curves of DOPO-HQ, OPPh₃, and THPPO. DOPO-HQ decomposed in one single step at 347 °C without any residue. THPPO underwent a multi-step decomposition and retained a residue yield of 14.6%, while OPPh₃ evaporated without residue at 245 °C. The decomposition started at 285 °C for DOPO-HQ, 299 °C for THPPO and at 307 °C for PDTT. PDTT's main decomposition

Table 1. Thermogravimetric results for PDTT, DOPO-HQ, OPPh$_3$, THPPO, EP, EP + PDTT, EP + DOPO-HQ, and EP + OPPh$_3$: temperature of 5 wt% mass loss ($T_{5wt\%}$), peak mass loss rate (PMLR), temperature of peak mass loss rate (T_{PMLR}), and residue yield at 900 °C.

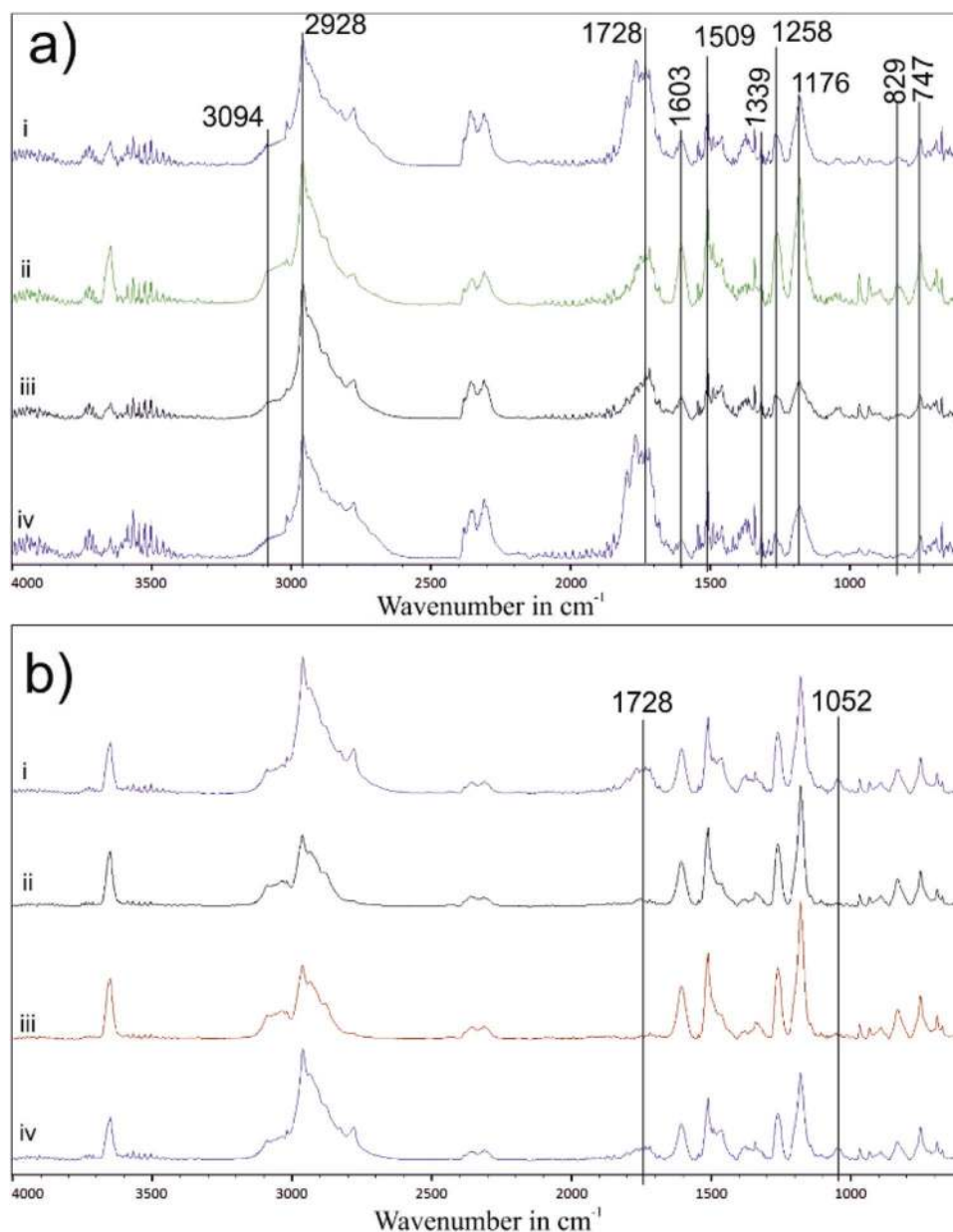| Material	P-content [wt%]	$T_{5wt\%}$ [°C ± 2]	PMLR [wt% s^{-1} ± 0.02]	T_{PMLR} [°C ± 2]	Residue [wt% ± 1]
PDTT	6.02	307	0.19	501	43.9
DOPO-HQ	9.55	285	0.34	347[a]	0.1
THPPO	9.49	299	0.12	329	14.6
OPPh$_3$	11.13	218	0.39	294	–
EP	–	346	0.30	372	9.5
EP + PDTT	0.60	320	0.23	365	10.3
EP + DOPO-HQ	0.96	326	0.27	366	9.0
EP + OPPh$_3$	1.11	292	0.21	367	10.5

[a]Uncertainty of ±4 °C.

step was at 501 °C, vastly higher than those of DOPO-HQ (347 °C) and THPPO (329 °C), thereby highlighting the superior stability of PDTT due its polymeric structure (Figure 3b).

EP decomposed in one one-step with a peak mass loss rate (PMLR) of 0.30 wt% s^{-1} at 373 °C and a residue of 9.5 wt% (Figure 3c). The temperature at 5 wt% mass loss ($T_{5wt\%}$) of EP was 346 °C, and this value was moderately reduced for EP + PDTT and EP + DOPO-HQ by 26 °C and 20 °C, respectively, and greatly reduced for EP + OPPh$_3$ by 54 °C, thereby correlating to the thermal stability of the flame retardants. While the temperatures at peak mass loss (T_{PMLR}) of EP + PDTT, EP + DOPO-HQ, and EP + OPPh$_3$ were almost unchanged compared to EP (Figure 3d), the PMLR and the residue yields of EP + PDTT and EP + OPPh$_3$ were altered. EP + OPPh$_3$ exhibited a residue yield of 10.5 wt%, although 8.6 wt% would be the calculated yield if OPPh$_3$ had evaporated out of the material without interacting with the polymer matrix. This observation, as well as the significantly lowered PMLR for EP + OPPh$_3$, distinctively proves an interaction between EP and OPPh$_3$ during the decomposition. For EP + PDTT, the residue was slightly increased compared to EP, but less so than expected: Assuming no relevant charring or interaction between EP and PDTT would take place, EP + PDTT would have a calculated residue yield of 13 wt% (8.6 wt% for nine parts EP and 4.4 wt% for one part PDTT). The notable difference between the expected residue of 13.0 wt% and the
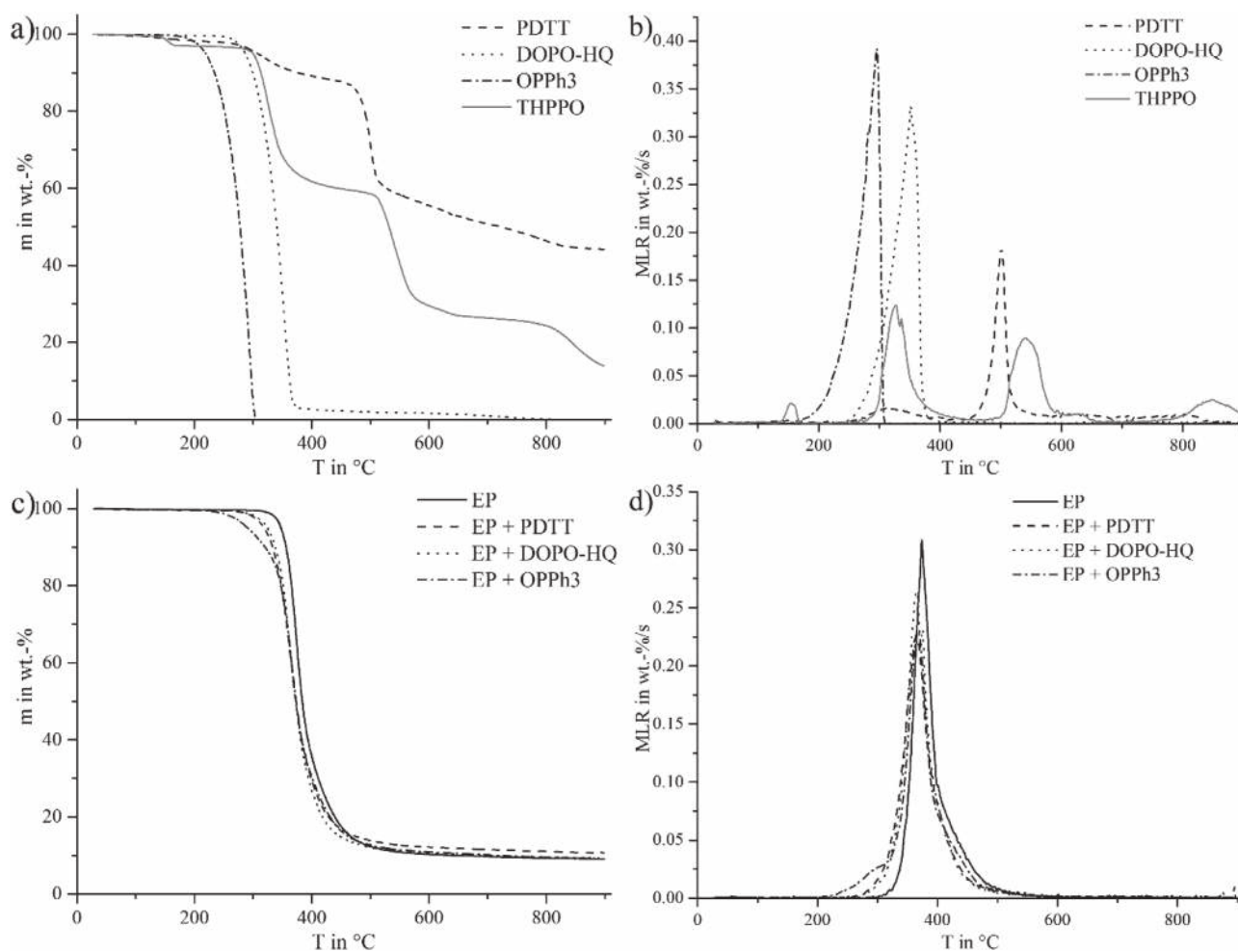
Figure 3. a)Thermal decomposition and b) mass loss rate of PDTT, DOPO-HQ, OPPh$_3$ and THPPO; c) thermal decomposition and d) mass loss rate of EP, EP + PDTT, EP + DOPO-HQ, and EP + OPPh$_3$

2000731 (5 of 12)

**ADVANCED
SCIENCE NEWS**

www.advancedsciencenews.com

**Macromolecular
Materials and Engineering**

www.mme-journal.de

Figure 4. TG-FTIR gas-phase spectra a) at the beginning of decomposition and b) during main decomposition step of i) EP, ii) EP+PDTT, iii) EP+DOPO-HQ, and iv) EP+OPPh$_3$.

measured residue of 10.3 wt% implies that there was no charring interaction between EP and PDTT during the pyrolytic decomposition of EP + PDTT. Moreover, it is conceivable that some EP decomposition products enhanced the decomposition of PDTT, which is susceptible to hydrolysis reactions, especially the (DOPO-) hydroquinone–terephthalic ester moieties. The reduced residue yield is also explained by the large discrepancy between the decomposition temperature ranges of matrix and flame retardant. Generally, a greater overlap in decomposition temperature ranges leads to greater chemical interaction of matrix, flame retardant, and their respective decomposition products.[22,48] A similar lack of charring trend was observed for aromatic hyperbranched polyphosphates, where the pure flame

retardant exhibited a high residue yield in TGA measurements, but failed to interact with the matrix in resin blends, leading to low residue yields in TGA overall poor flame retardancy performance.[28]

The evolved gas FTIR spectra of EP and the flame retardant-containing samples are displayed in **Figure 4**. The spectra in Figure 4a corresponds to the decomposition products at the beginning of decomposition, while Figure 4b displays the products at the main decomposition step. Notably, the spectra in Figure 4b largely resembled the decomposition products of the epoxy resin matrix.

The key signals consistent with signals from bisphenol A were the band at 3649 cm^{-1}, the wide band at 3094 cm^{-1}, the

strong band at 2928 cm^{-1}, the two bands at 1603 and 1509 cm^{-1}, the small band at 1339 cm^{-1}, the two sharp bands at 1258 and 1176 cm^{-1}, and the two bands at 829 and 747 cm^{-1}. These signals have been extensively described in detail elsewhere.[28] Moreover, the two bands at 967 and 931 cm^{-1} were indicative of the evolution of ammonia stemming from the hardener IPDA. Noteworthy was the lack of signal at 1728 cm^{-1} for EP + PDTT and EP + DOPO-HQ. This band corresponds to $\nu(C = O)$, indicating that the interaction of flame retardant and matrix led to a reduced production of carbonyl-containing species like acetaldehyde or acetone, products of EP decomposition. Additionally, the spectra of EP + PDTT and EP + DOPO-HQ in Figure 4b did not exhibit absorbance at 1052 cm^{-1}, which are associated with secondary hydroxyl groups of the epoxy resin resultant of the ring-opening of the epoxide moiety during curing. The lack of these signals provided evidence of some chemical interaction of flame retardant and matrix. In Figure 4a, the spectra of all flame retardant-containing materials strongly resembled the spectra of the epoxy resin matrix. Notably, EP + PDTT exhibited strong bisphenol A and ammonia signals, the latter being stronger than for any other material. This was caused by a shift in decomposition pathway when PDTT was present. Moreover, the $\nu(C = O)$ band at 1728 cm^{-1} was lower in intensity for EP + DOPO-HQ and EP + PDTT, further pointing toward an interaction leading to reduced carbonyl-species production. Previous investigations of the decomposition routes of the epoxy resin have pointed out that the pathways may be divergent and dependent on the heating rate (high temperatures favor chain scission reactions);[49] moreover, the secondary alcohol groups may decompose to form carbonyl-functionalized products such as acetone or acetaldehyde. The presence of PDTT and PDTT's decomposition products had an influence on the decomposition pathway of EP, for example through reactions like Fries-rearrangement of terephthalic ester moieties leading to reactive hydroxyl groups, and effects of flame retardants affecting the decomposition pathway of the matrix have been previously investigated.[48,50] The secondary alcohol groups may be phosphorylated by the flame retardant or its decomposition products, leading to a reduction of available secondary alcohols in the matrix, which explains the lower concentration of these signals as well as those of acetaldehyde in FTIR measurements of these specimens. Moreover, the presence of DOPO-moieties led to a decrease in residue for EP + DOPO-HQ compared to EP, indicating that the presence of DOPO interfered with the decomposition pathway and charring mechanism. Thus, the evolved gas spectra of decomposition products from flame retardant-containing resins highlighted that the presence of PDTT led to an alternate pathway of matrix decomposition compared to other flame retardants, exemplified by the lowered acetaldehyde and secondary hydroxyl production of the resin.

2.6. Investigation Via Pyrolysis Combustion Flow Calorimeter (PCFC)

The results of PCFC measurements are summarized in **Table 2**. Due to the measurement principle of PCFC, whereby pyrolytic decomposition products are completely oxidized in a

Table 2. PCFC results for EP, EP + PDTT, EP + DOPO-HQ, and EP + OPPh$_3$: heat release capacity (HRC), total heat evolved (THE), temperature of highest oxygen consumption (T_{maxOx}), and residue.

| Material	P-content [wt%]	HRC [J g^{-1} K^{-1} ± 10]	THE [kJ g^{-1} ± 0.5]	T_{maxOx} [°C ± 2]	Residue [wt% ± 1]
EP	–	498	28.9	387	6.4
EP + PDTT	0.60	404	28.1	377	7.4
EP + DOPO-HQ	0.96	446	28.9	379	6.8
EP + OPPh$_3$	1.11	442	29.0	386	5.8

combustor, the results do not provide information on radical scavenging, which is key for materials dependent on this gas phase mode of action such as phosphorus-based flame retardants and especially DOPO-based materials. However, PCFC provides insight into the release of incombustible gases and changes in the heats of combustion of the volatiles.

EP exhibited a heat release capacity (HRC) of approx. 500 J g^{-1} K^{-1}, its temperature of maximum oxygen consumption (T_{maxOx}) was 387 °C, and it had a total heat evolved (THE) of 28.9 kJ g^{-1}. EP + PDTT, EP + DOPO-HQ, and EP + OPPh$_3$ showed little impact on THE and T_{maxOx} compared to EP, but they impacted the heat release capacity (HRC). While the EP + DOPO-HQ and EP + OPPh$_3$ exhibited a reduction of roughly 10%, an almost 20% reduction in HRC was observed for EP + PDTT. These results point to the release of incombustible gases for EP + PDTT and EP + DOPO-HQ, which correlates well with the findings in the evolved gas analysis via TG-FTIR. The increased evolution of ammonia seen in gas phase FTIR measurements highlight the flame dilution potential of these materials, as the release of incombustible materials affects HRC.

The residue yield was barely altered for EP + DOPO-HQ and EP + OPPh$_3$ compared to EP, but an increase in the case of EP + PDTT was noticeable. These observations indicate that PDTT can, to a limited extent, act as flame retardant in the condensed phase, although its primary mode of action is flame inhibition and flame dilution in the gas phase, as derived from TG-FTIR measurements and changes in the HRC. Generally, PCFC results pointed to very few changes of the flame retardants to EP in terms of charring and fuel dilution.

The residue yields of EP, EP + PDTT, EP + DOPO-HQ, and EP + OPPh$_3$ all differ by 2 to 5 wt% from the respective residue amounts in TGA investigations. This observation is explained by the sixfold higher heating rate used in PCFC (60 °C min^{-1}, versus 10 °C min^{-1} in TGA). The higher heating rate in PCFC is chosen to simulate the typical heating rates in burning polymeric specimens.[51–53] It has been demonstrated that the decomposition behavior of epoxy-based materials and other polymers, for example polyesters and polysiloxanes, is dependent on the applied heating rate.[49,54–59] To illustrate the influence of the heating rate, the mass loss of EP at 900 °C was determined for a number of heating rates between 0.5 °C min^{-1} and 60 °C min^{-1}. The results are displayed in **Figure 5**. The curve shows a distinctive correlation between heating rate and residue, with a higher heating rate resulting in a lower amount of residue.

The heating rate also influences the decomposition of the flame retardants and their interaction with the polymer matrix, as evidenced by EP + OPPh$_3$, which exhibits the largest
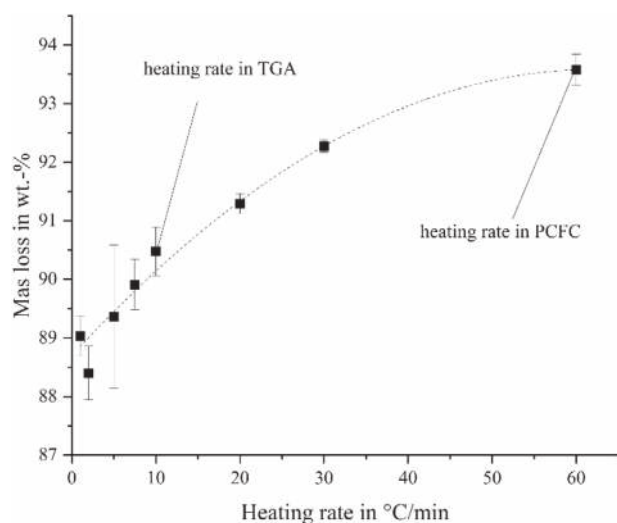
Figure 5. Mass loss of EP at 900 °C for different heating rates.

difference in residue yield (almost 5 wt%) between PCFC and TGA. During the PCFC investigation at 60 K min⁻¹, EP + OPPh₃ exhibited a residue yield of 5.8 wt% (exactly 90% of the residue of EP), suggesting that OPPh₃ evaporated out of the material without interacting with the polymer matrix. In contrast, during the TGA investigation at 10 K min⁻¹, EP + OPPh₃ exhibited 10.5 wt.% residue, distinctively more than for pure EP. OPPh₃ evidently increased the residue yield of EP at 10 K min⁻¹, but not at 60 K min⁻¹, proving a distinctive influence of the heating rate on the interaction between flame retardant and polymer matrix during the decomposition, that is, a shift in the decomposition pathway of the matrix.

2.7. Reaction to Small Flame (UL 94)

Table 3 summarizes the results of the UL 94 investigation of the materials. Due to the low flame retardant loading, no system achieved a vertical rating. EP + PDTT, EP + DOPO-HQ, and EP + OPPh₃ were all classified with HB-rating, the same as EP. The horizontal burning speed was hardly improved for EP + PDTT as well as EP + DOPO-HQ compared to EP, and only a slight improvement for EP + OPPh₃ occurred. The P-content in EP + PDTT (0.7 wt%) was not sufficiently high to achieve good flammability protection of the epoxy resin matrix. Notably, EP + OPPh₃ achieved the lowest horizontal burning rate due to the vaporization of the flame retardant from the matrix already at

Table 3. UL 94 results for EP, EP + PDTT, EP + DOPO-HQ, and EP + OPPh₃ (horizontal burning rates given with standard deviation).

Material	P-content [n wt%]	UL 94	burning rate [mm min⁻¹]
EP	–	HB	25 ± 2
EP + PDTT	0.60	HB	23 ± 3
EP + DOPO-HQ	0.96	HB	23 ± 2
EP + OPPh₃	1.11	HB	20 ± 1

low temperatures, relating to its gas phase action. Moreover, the P-content of EP + OPPh₃ is higher than that of EP-PDTT by a factor of 1.85.

2.8. Forced Flaming Behavior

Table 4 displays the results of cone calorimeter measurements of the epoxy resin samples, while **Figure 6** shows the corresponding heat release rate (HRR)-time curves. EP exhibited a total heat evolved (THE) of about 76 MJ m⁻² and a peak heat release rate (PHRR) of approx. 1000 kW m⁻². The shape of the HRR curve corresponds to an intermediate thick non-charring material.[60] After ignition, the material quickly reached its PHRR at about 120 s after the start of test, and the HRR rapidly declined thereafter. The quasi-static HRR, which corresponds to a steady state HRR, is only visible as a slight shoulder in the HRR curve after ignition, and it disappears shortly before reaching PHRR. After approx. 180 s, a local peak in HRR was observed in the HRR plots, which relates to the burning of the epoxy resin under the retained frame. EP burned with an effective heat of combustion (EHC = total heat evolved / total mass loss) of 24.4 MJ kg⁻¹ and its residue yield was about 8 wt%.

The incorporation of PDTT, DOPO-HQ, and OPPh₃ to EP all led to a reduction in the ignition time by about 15 s compared to EP. This behavior is typical when incorporating flame retardants into EP and is related to a lower cross-link density of the matrix.[61] Overall, the shape of the HRR curves for flame retardant mixtures remained similar to EP, in that the PHRR was reached quickly after ignition, followed by a sharp decline and a plateau leading toward flame out. The flame retardancy potential of OPPh₃ was the least impactful on improving the fire behavior of EP: EP + OPPh₃ exhibited an 18% reduction in THE, 16% in PHRR, and 11% reduction of the maximum average rate of heat emission (MARHE) compared to EP. Although EP + OPPh₃ contained the highest P amounts among

Table 4. Cone calorimeter results for EP, EP + PDTT, EP + DOPO-HQ, and EP + OPPh₃: time to ignition (t_{ig}), total heat evolved (THE), peak heat release rate (PHRR), total mass loss (TML), effective heat of combustion (EHC), total smoke release (TSR), carbon monoxide yield (COY) 2 min after ignition, fire growth rate (FIGRA), and maximum average rate of heat emission (MARHE).
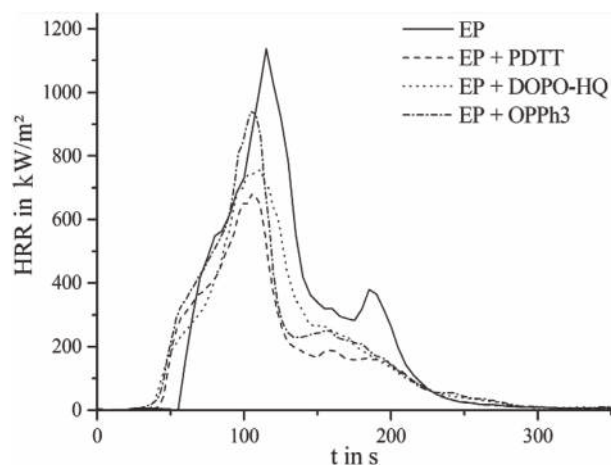
Material	P-content [n wt%]	t_{ig} [s ± 2]	THE [MJ m⁻² ± 5]	PHRR [kW m⁻² ± 80]	TML [wt% ± 1]
EP	–	54	75.8	1068	92.1
EP + PDTT	0.60	40	56.0	736	89.9
EP + DOPO-HQ	0.96	40	59.6	725	84.3
EP + OPPh₃	1.11	38	62.5	900	91.6

Material	EHC [MJ kg⁻¹]	TSR [m² m⁻² ± 100]	COY [kg kg⁻¹ ± 0.02]	FIGRA [kW s⁻¹ m⁻²]	MARHE [kW m⁻²]
EP	24.4	2720	0.0620	9.7	390
EP + PDTT	19.2	3597[a]	0.1096	8.8	308
EP + DOPO-HQ	21.1	3338	0.1652	7.1	309
EP + OPPh₃	20.4	3934	0.1623	8.8	345

[a]Uncertainty of ±540 m² m⁻²

**ADVANCED
SCIENCE NEWS**
www.advancedsciencenews.com

**Macromolecular
Materials and Engineering**
www.mme-journal.de

Figure 6. Heat release rate over time for EP, EP + PDTT, EP + DOPO-HQ, and EP + OPPh₃.

the tested flame retardants, the addition of OPPh₃ to EP led to the highest THE, PHRR, total mass loss (TML), and MARHE of all tested flame retardants. In addition, EP + OPPh₃ showed the highest smoke production of all materials in this study at almost 4000 m² m⁻². TGA measurements pointed to the volatility of OPPh₃, and this volatility is linked to a gas phase mode of action which was quantifiable in cone calorimeter measurements of EP + OPPh₃ via changes in EHC, carbon monoxide yield (COY), and total smoke release (TSR). EHC is a parameter of gas phase activity,[48] and the addition of OPPh₃ into EP lowered the EHC of the resin by 16%, but did not lead to changes in mass loss. Hence, it follows that the main mode of action of OPPh₃ is in the gas phase, that is flame inhibition via radical scavenging. The main contributor to heat release is the formation of carbon dioxide (CO_2) from the reaction of carbon monoxide (CO) with a hydroxyl radical. The radical scavenging effect of P in the gas phase leads to an increase in COY, as the hydroxyl radicals are replaced by less reactive P-species. This mode of action affects the combustion efficiency of the flame, leading to greater incomplete combustion and higher smoke release. Notably, the COY of EP + OPPh₃ was 2.6 times higher than that of EP and the TSR was 1.5 times higher, thereby highlighting the gas phase mode of action of this flame retardant. A similar conclusion can be made for the other flame retardants, as they also exhibited an increase in COY and TSR as well as a decrease in EHC compared to EP, thereby pointing to gas phase modes of action.

The addition of DOPO-HQ to EP reduced THE by 21%, PHRR by 31%, and the MARHE-value by 21% compared to EP. Moreover, the fire growth rate (FIGRA = max (HRR/t)) of EP was lowest when DOPO-HQ was added. The EHC was decreased by only 13%, the least impactful change compared to the other flame retardants, although the addition of DOPO-HQ to EP led to the highest residue yields among tested flame retardants. The increase in char, as well as the decrease in the FIGRA, implied a moderate gas as well as condensed phase activity of DOPO-HQ.[26] The flame inhibition effect of DOPO-HQ was also evident from several short flashes that occurred before sustained ignition of EP + DOPO-HQ.

Although it had the lowest P-content of all tested flame retardants, the incorporation of PDTT exhibited the greatest improvement to the fire performance of EP. The PHRR and MARHE of EP + PDTT were on a similar level to EP + DOPO-HQ, however THE was reduced by 26% compared to EP, which was 3.6 MJ m⁻² less than EP + DOPO-HQ. The EHC was notably reduced by 21% and the residue yield did not greatly decrease compared to EP, thereby pointing to a strong gas phase mode of action. This is underscored by the strong smoke production compared to EP. The CO-yield was the lowest for EP + PDTT (0.11 kg kg⁻¹) compared to EP + DOPO-HQ and EP + OPPh₃ (around 0.16 kg kg⁻¹, respectively), however, EP + PDTT also had the lowest P-content among the tested materials.

For EP + PDTT, EP + DOPO-HQ, and EP + OPPh₃, the percental reduction in PHRR was not vastly higher than the percental reduction in THE compared to EP (less than 10% difference, respectively), indicating the absence of strong barrier effects. All materials in this study showed no visible intumescence and generally formed only moderate amounts of residue in the cone calorimeter investigation (**Figure 7**), mainly along the edge of the retained frame. The increase in char for EP + DOPO-HQ and EP + PDTT offered some protective layer effects made evident by the decrease in PHRR compared to EP due to the high content of aromatic groups, particularly in PDTT. Moreover, the HRR curves in Figure 6 illustrate that the addition of flame retardants to EP led to the disappearance of the local maximum near 200 s. The evolution of moderate charring hindered extensive combustion of the material under the retainer frame, which, in combination of a pronounced gas phase mode of action, ultimately lowered the fire load of EP + DOPO-HQ and EP + PDTT.

Elemental analysis of the residues revealed that most of the original phosphorus content in the resin blends was lost during combustion (**Table 5**). This observation provided further evidence that the flame retardants in this study were predominantly active in the gas phase. The phosphorus content remaining in the residue was 20% for EP + PDTT, 26% for EP + DOPO-HQ, and only 6% for EP + OPPh₃. Especially the elevated P-content in EP + DOPO-HQ and EP + PDTT point to a condensed phase mode of action of the flame retardants, whereby P acts as a net-point between aromatic moieties, thus fixing fuel in the condensed phase. This correlates well with the increase in residue yields in cone calorimeter, as well as the reduced PHRRs.

3. Conclusions

A polymeric phosphorus-containing flame retardant with a complex rigid structure and phosphorus structure elements of two different chemical environments was synthesized and investigated in an epoxy resin. With only 10 wt% loading (0.6 wt% phosphorus-content), EP + PDTT exhibited good performance in cone calorimeter investigation with a 25% reduction in THE and a 30% reduction in PHRR compared to EP. PDTT acted predominantly in the gas phase via flame inhibition, as evidenced by its impact on key flame retardancy parameters, for example a 21% reduction in EHC. The overall performance of PDTT in EP was comparable to or better than

Figure 7. Cone calorimeter residues of a) EP, b) EP + PDTT, c) EP + DOPO-HQ, and d) EP + OPPh$_3$.

DOPO-HQ (0.96 wt% P) regarding UL 94 and most parameters in cone calorimeter testing and PCFC. However, EP + PDTT showed a much lower CO-yield and notably lower HRC than EP + DOPO-HQ. In contrast to OPPh$_3$, PDTT did not deteriorate the T_g of EP, but greatly increased it due to its reinforcing effect in epoxy resins resulting from its rigid, aromatic shape.

The remarkable performance at low loading and toughening effect make PDTT a promising flame retardant for EP and potentially multiple other engineering plastics.

4. Experimental Section

Materials and Methods: Unless stated otherwise, all raw materials were purchased from commercial sources and used as received without further purification.

9,10-Dihydro-9-oxa-10-phosphaphenanthrene-10-oxide (DOPO) was purchased from TCI Europe (purity >97%). 1,4-terephtaloyl chloride (TPC), *p*-bromoanisole, *p*-benzoquinone, magnesium, phosphorus

trichloride, potassium permanganate, boron tribromide, triethylamine (Et$_3$N), and 4-*N*,*N*-dimethylaminopyridine (DMAP) were purchased from Sigma–Aldrich with a purity of at least 99%. All solvents, namely dichloromethane (DCM), ethanol, cyclohexane, and ethoxyethanol, were at least of reagent grade quality. Tetrahydrofuran (THF) for the synthesis of THPPO was distilled in a benzophenone-sodium still. Water was purified with a Sartorius ultrapure water system.

Diglycidyl ether of bisphenol A (DGEBA, Araldite MY740) was purchased from Bodo Möller Chemie GmbH (Offenbach, Germany) and isophorone diamine (IPDA) from Merck (Darmstadt, Germany). Triphenylphosphine oxide was purchased from Sigma–Aldrich Laborchemikalien GmbH (Seelze, Germany).

^{1}H and ^{31}P-NMR spectra were recorded on a Bruker Avance 600 spectrometer (Bruker Biospin, Rheinstetten, Germany).

ESI-TOF was measured on an Agilent 6210 ESI-TOF (Agilent Technologies, Santa Clara, CA, USA). The solvent flow rate was adjusted to 10 µL min^{-1}, and the spray voltage set to 4 kV. Drying gas flow rate was set to 30 psi (≈2 bar). The samples were dissolved in methanol and measured with a fragmentor voltage of 250 V in positive mode. All other parameters were adjusted for a maximum abundance of the relative [M+H]$^+$.

Elemental analysis (C, P, H) was done by Mikroanalytisches Laboratorium Kolbe (Mühlheim an der Ruhr, Germany).

ATR-FTIR spectra were recorded by using Nicolet 8700 Thermo Scientific spectrometer with smart orbit diamond cryo 2012 equipped with an IR light source, and an MCT / A detector in the range of 650 to 4000 cm^{-1}. The measurements were performed using Omnic version 7.3 software (Thermo Electron Corporation) and each spectrum was the average of 60 scans with a measurement time of 60 s and a resolution of 4000 cm^{-1} using auto baseline correction.

Differential scanning calorimetry (DSC) was performed on a DSC 204 F1 from NETZSCH (Selb, Germany). Two heating cycles ranging from 20 °C to 220 °C were applied to a sample mass of 12 ± 1 mg.

Table 5. Phosphorus contents of unburnt material and residue for EP + PDTT, EP + DOPO-HQ, and EP + OPPh$_3$.

Material	P-content neat material [wt%]	P-content residue [wt%]	Remnant of original P-content [%]
EP + PDTT	0.60	1.88	20.26
EP + DOPO-HQ	0.96	2.21	26.09
EP + OPPh$_3$	1.11	0.90	6.09

For thermogravimetric analysis (TGA), a TG 209 F1 Iris from NETZSCH (Selb, Germany) was used. A sample of 10.0 ± 0.1 mg was heated from 30 °C to 900 °C, applying a heating rate of 10 °C min⁻¹ under nitrogen. Two measurements were performed and averaged for each material. For TG-FTIR, the device was coupled with a Tensor 27 (Bruker, Germany), while the transfer line and gas cell were heated to 250 °C to avoid condensation of the pyrolysis products.

UL 94 vertical and horizontal testing was performed in a fire chamber from Fire Testing Technology (FTT, East Grinstead, UK), in accordance to IEC 60695-11-10. Specimens of 13 mm width and 3 mm thickness were used.

For pyrolysis combustion flow calorimeter (PCFC), an FTT (East Grinstead, UK) FAA Micro Calorimeter was used, applying a heating rate of 1 °C s⁻¹ from 150 °C to 750°C to a sample weight of 5 ± 0.1 mg. Two measurements were performed and averaged for each material. Cone calorimeter investigation was performed with an FTT (East Grinstead, UK) cone calorimeter in accordance to ISO 5660. A heat flux of 50 kW m⁻² was applied with a distance between heating cone and specimen of 35 mm.[27] Samples were measured using a retainer frame upon which an additional thin wire cross was fastened to prevent the samples from rearing up. Results were calculated for a sample surface area of 100 cm² despite the retainer frame, as the specimens burned beneath the frame at the edges. The flame-out was declared when the smoke production dropped below 0.01 m² s⁻¹ in order to establish a consistent reference point. Two measurements were performed and averaged for each material.

Synthesis: Spectroscopic and analytical data is provided in the Supporting Information. These are sorted as follows: Figures S1 and S2, Supporting Information, exhibit the ESI-TOF measurements of DOPO-HQ and THPPO, respectively. In Figure S3, Supporting Information, the ¹H and ¹H[³¹P-decoupled]-NMR spectra of DOPO-HQ are displayed, while Figure S4, Supporting Information, shows the ¹H-NMR of THPPO. In Figure S5, Supporting Information, the ¹H-NMR spectra of DOPO-HQ, THPPO, and PDTT are compared. The ¹H-NMR of PDTT is shown in greater detail in Figure S6, Supporting Information, while Figure S7 and Figure S8, Supporting Information, display the ¹H,¹H-COSY-NMR and ¹³C{¹H}-NMR spectra of this material. Additionally, Figure S9, Supporting Information, plots the H,C-HSQC and the HC-HMBC spectra of PDTT. The ³¹P{¹H}-NMR spectrum is exhibited in Figure S10, Supporting Information, and the ³¹P{¹H}-NMR spectra of DOPO-HQ and PDTT are compared in Figure S11, Supporting Information.

Monomer Synthesis: 10-(2,5-Dihydroxyphenyl)-10H-9-oxa-10-phosphaphenanthrene-10-oxide (DOPO-HQ) was synthesized as described by Wang et al.[35] in one step from 9,10-dihydro-9-oxa-10-phosphaphenanthrene-10-oxide (DOPO): in a 2 L round-bottomed flask with attached reflux condenser and overhead stirrer, *p*-benzoquinone was incrementally added to a solution of DOPO in ethoxyethanol. The mixture was heated to 125 °C and allowed to react for 4 h, and subsequently collected by filtration at room temperature (RT) and recrystallized in ethoxyethanol to receive DOPO-HQ. The obtained characterization data were in accordance with the literature: ¹H NMR (Figure S3, Supporting Information) (600 MHz, DMSO-d6, δ): 6.60 (t, 1H), 6.85 (dd, 1H), 7.14 (dd, 1H), 7.22–7.30 (m, 2H), 7.38–7.51 (m, 2H), 7.54–7.72 (m, 2H), 8.18–8.23 (m, 2H) (under 5 ppm, residual ethoxyethanol); ³¹P NMR (Figure S9, Supporting Information) (600 MHz, CDCl₃, δ): 17.1 ppm; HRMS (Figure S1, Supporting Information) *m/z*: [M + H]⁺ calculated for C₁₈H₁₂NaO₄P, 347.04; found 347.05 (cf. Supplemental Information).

Tris(4-hydroxyphenyl)phosphine oxide (THPPO) was synthesized in three steps according to the procedure of Whitlock et al.[34] First, tri-*p*-anisylphosphine was prepared according to the procedure of Mann and Chaplin,[62] where *p*-bromoanisol was allowed to react with phosphorus trichloride via Grignard reaction. Next, tri-*p*-anisylphosphine was oxidized by the reaction with potassium permanganate in water to form tris(4-methoxyphenyl)phosphine oxide. In the last step, THPPO was prepared via deprotection of the previously obtained tris(4-methoxyphenyl)phosphine oxide using boron tribromide in DCM. The obtained characterization data were in accordance with the literature.

¹H NMR (Figure S4, Supporting Information) (600 MHz, Acetone-d6, δ): 7.40 (dd, 6H, C(2)H), 7.05 (dd, 6H, C(3)H); HRMS (Figure S2, Supporting Information) *m/z*: [M + H]⁺ calculated for C₁₈H₁₅NaO₄P, 349.05; found 349.06. (cf. Supporting Information).

Synthesis of the Polymer PDTT: For the synthesis of poly-(DOPO-HQ/THPPO-terephthalate) (PDTT), a procedure similar to the one described by Ranganathan, Emrick et al. was implemented.[63] In a 2 L round-bottomed flask equipped with a reflux condenser, an addition funnel, and stir bar, DOPO-HQ (19.92 g, 61.4 mmol, 1.00 eq.) and THPPO (1.0 g, 3.1 mmol, 0.05 eq.) were suspended in a mixture of anhydrous dichloromethane (300 mL) and anhydrous triethylamine (23 mL, 165 mmol, 2.7 eq.). To this suspension, DMAP (0.2 g, 1.64 mmol, 0.03 equiv.) was added, and the flask was placed in an ice bath. A solution of terephthaloyl chloride (13.34 g, 65.7 mmol, 1.07 eq.) in DCM (200 mL) was added dropwise with an addition funnel over the timespan of 20 min to the vigorously stirred reaction mixture (750 rpm). The reaction mixture was stirred for 2 h at RT, followed by 2 h at reflux. The mixture was then allowed to cool to RT, concentrated to 100 mL, and poured into 1 L cold water. The precipitate was collected by filtration, washed with water, and dried at reduced pressure. The slightly ochre crude product (30.5 g) was further purified by Soxhlet extraction in water (14 h, followed by drying at 80 °C for 2 days in vacuo, 28.5 g) and chlorobenzene (14h, followed by drying at 80 °C for 2 days at reduced pressure, 14.0 g). PDTT was obtained as a white solid.

¹H-NMR (Figure S6, Supporting Information) (400 MHz, CDCl₃, δ): 1.14–1.20 (m, 3H), 1.34 (t, 4H), 3.03 (sext, 3H), 3.49–3.55 (m, 2H), 3.69–3.72 (m, 2H), 4.41–4.43 (m, 2H), 6.9–7.1 (m, 2H) 7.2 (s, 1H), 7.2–7.4 (m, 4H), 7.45–7.75 (m, 6H), 7.8–7.9 (m, 1H), 8.04 (s, 1H), 8.15–8.35 (m, 3H)

³¹P-NMR (Figure S10, Supporting Information) (600 MHz, CDCl₃, δ): 17.1, 18.02–18.05, 27.8 ppm; IR: ν = 3065 (w, C—H arom), 1735 (s, C=O ester), 1595 (w, C=C), 1583 (w, C=C), 1475 (m, P—C arom), 1448 (w), 1431 (w), 1402 (w), 1235 (s, P=O), 1201 (m, C—O ester), 1174 (s, P—O arom),[64] 1118 (m, P=O), 1061 (s, C—O ester), 1013 (s), 917 (m, P—O—C arom),[64] 872 (m), 780 (w), 755 (s, C—H arom bend.), 715 (s, C—H arom bend.), 673 (w), 617 (w), 605 (m), 550 (w), 519 (m), 507 (m), 496 (m), 423 (w) cm⁻¹.

Supporting Information

Supporting Information is available from the Wiley Online Library or from the author.

Conflict of Interest

The authors declare no conflict of interest.

Data Availability Statement

Data available on request from the authors.

[1] S. Kemmlein, O. Hahn, O. Jann, *Atmos. Environ.* **2003**, *37*, 5485.

[2] M. M. Velencoso, A. Battig, J. C. Markwart, B. Schartel, F. R. Wurm, *Angew. Chem., Int. Ed.* **2018**, *57*, 10450.

[3] L. Chen, Y.-Z. Wang, *Materials* **2010**, *3*, 4746.

[4] S. Brehme, T. Koppl, B. Schartel, O. Fischer, V. Altstädt, D. Pospiech, M. Döring, *Macromol. Chem. Phys.* **2012**, *213*, 2386.

[5] P. Müller, Y. Bykov, M. Döring, *Polym. Adv. Technol.* **2013**, *24*, 834.

[6] B. Perret, B. Schartel, K. Stöß, M. Ciesielski, J. Diederichs, M. Döring, J. Krämer, V. Altstädt, *Macromol. Mater. Engin.* **2011**, *296*, 14.

[7] L. Zang, S. Wagner, M. Ciesielski, P. Müller, M. Döring, *Polym. Adv. Technol.* **2011**, *22*, 1182.

[8] X. L. Chen, J. L. Zhuo, C. M. Jiao, *Polym. Degrad. Stab.* **2012**, *97*, 2143.

[9] X. L. Chen, C. M. Jiao, S. X. Li, J. Sun, *J. Polym. Res.* **2011**, *18*, 2229.

[10] Y. L. Chang, Y. Z. Wang, D. M. Ban, B. Yang, G. M. Zhao, *Macromol. Mater. Eng.* **2004**, *289*, 703.

[11] B. I. Voit, A. Lederer, *Chem. Rev.* **2009**, *109*, 5924.

[12] K. L. Wooley, C. J. Hawker, J. M. J. Frechet, *J. Chem. Soc., Perkin Trans. 1* **1991**, 1059.

[13] S. G. Gaynor, S. Edelman, K. Matyjaszewski, *Macromolecules* **1996**, *29*, 1079.

[14] L. Boogh, B. Pettersson, P. Kaiser, J. A. Manson, in *28th Int. SAMPE Technical Conf.*, SAMPE, Diamond Bar, CA **1996**, *28*, 236.

[15] C. J. Hawker, R. Lee, J. M. J. Frechet, *J. Am. Chem. Soc.* **1991**, *113*, 4583.

[16] K. E. Uhrich, C. J. Hawker, J. M. J. Frechet, S. R. Turner, *Macromolecules* **1992**, *25*, 4583.

[17] E. Stubbs, M. Brown, A. Steele, C. Song, T. Emrick, *J. Polym. Sci., Part A: Polym. Chem.* **2019**, *57*, 1765.

[18] Z. K. Yuan, J. H. Yu, B. L. Rao, H. Bai, N. Jiang, J. Gao, S. R. Lu, *Macromol. Res.* **2014**, *22*, 405.

[19] Q. F. Wang, W. F. Shi, *Polym. Degrad. Stab.* **2006**, *91*, 1289.

[20] D. Zhang, D. Jia, *J. Appl. Polym. Sci.* **2006**, *101*, 2504.

[21] A. Battig, J. Markwart, F. R. Wurm, B. Schartel, *Polym. Chem.* **2019**, *10*, 4346.

[22] A. Battig, J. C. Markwart, F. R. Wurm, B. Schartel, *Polym. Degrad. Stab.* **2019**, *170*, 108986.

[23] A. Battig, J. C. Markwart, F. R. Wurm, B. Schartel, *Eur. Polym. J.* **2020**, *122*, 109390.

[24] K. Täuber, F. Marsico, F. R. Wurm, B. Schartel, *Polym. Chem.* **2014**, *5*, 7042.

[25] J. C. Markwart, A. Battig, M. M. Velencoso, D. Pollok, B. Schartel, F. R. Wurm, *Molecules* **2019**, *24*, 3901.

[26] J. C. Markwart, A. Battig, T. Kuckhoff, B. Schartel, F. R. Wurm, *Polym. Chem.* **2019**, *10*, 5920.

[27] U. Braun, A. I. Balabanovich, B. Schartel, U. Knoll, J. Artner, M. Ciesielski, M. Döring, R. Perez, J. K. W. Sandler, V. Altstadt, T. Hoffmann, D. Pospiech, *Polymer* **2006**, *47*, 8495.

[28] J. C. Markwart, A. Battig, L. Zimmermann, M. Wagner, J. Fischer, B. Schartel, F. R. Wurm, *ACS Appl. Polym. Mater.* **2019**, *1*, 1118.

[29] B. Schartel, U. Braun, A. I. Balabanovich, J. Artner, M. Ciesielski, M. Döring, R. M. Perez, J. K. W. Sandler, V. Altstädt, *Eur. Polym. J.* **2008**, *44*, 704.

[30] X. M. Zhao, H. V. Babu, J. Llorca, D. Y. Wang, *R.Adv* **2016**, *6*, 59226.

[31] M. Ciesielski, A. Schäfer, M. Döring, *Polym. Adv. Technol.* **2008**, *19*, 507.

[32] M. Ciesielski, J. Diederichs, M. Döring, A. Schäfer, in *Fire and Polymers V: Materials and Concepts for Fire Retardancy* (Eds: C. A. Wilkie, A.B. Morgan, G. L. Nelson), Vol. 1013, American Chemical Society, Washington, D.C. **2009**, p. 174.

[33] B. Schartel, J. H. Wendorff, *Polym. Eng. Sci.* **1999**, *39*, 128.

[34] B. P. Friedrichsen, D. R. Powell, H. W. Whitlock, *J. Am. Chem. Soc.* **1990**, *112*, 8931.

[35] C.-S. Wang, J.-Y. Shieh, *Polymer* **1998**, *39*, 5819.

[36] L. Qian, J. Zhi, B. Tong, J. Shi, F. Yang, Y. Dong, *Polymer* **2009**, *50*, 4813.

[37] X. C. Bian, L. Chen, J. S. Wang, Y. Z. Wang, *J. Polym. Sci., Part A: Polym. Chem.* **2010**, *48*, 1182.

[38] O. Fischer, D. Pospiech, A. Korwitz, K. Sahre, L. Häussler, P. Friedel, D. Fischer, C. Harnisch, Y. Bykov, M. Döring, *Polym. Degrad. Stab.* **2011**, *96*, 2198.

[39] C. H. Lin, J. C. Chen, C. M. Huang, J. M. Jehng, H. C. Chang, T. Y. Juang, W. C. Su, *Polymer* **2013**, *54*, 6936.

[40] X. Wang, Y. Hu, L. Song, W. Y. Xing, H. D. A. Lu, P. Lv, G. X. Jie, *Polymer* **2010**, *51*, 2435.

[41] Z. R. Fan, A. Lederer, B. Voit, *Polymer* **2009**, *50*, 3431.

[42] T. Zhang, B. A. Howell, P. B. Smith, *Ind. Eng. Chem. Res.* **2017**, *56*, 1661.

[43] P. Lautenschlager, J. Brickmann, J. Vanruiten, R. J. Meier, *Macromolecules* **1991**, *24*, 1284.

[44] B. Schartel, V. Stümpflen, J. Wendling, J. H. Wendorff, W. Heitz, R. Neuhaus, *Colloid Polym. Sci.* **1996**, *274*, 911.

[45] D. J. Plazek, Z. N. FrundJr., *J. Polym. Sci., Part B: Polym. Phys.* **1990**, *28*, 431.

[46] F. Kempel, B. Schartel, J. M. Marti, K. M. Butler, R. Rossi, S. R. Idelsohn, E. Oñate, A. Hofmann, *Fire Mater.* **2015**, *39*, 570.

[47] E. H. Immergut, H. F. Mark, in Plasticization and Plasticizer Processes (Ed: N.A.J. Platzer), *Advances in Chemistry*, Vol. *48*, ACS Publications, Washington, D.C **1965**.

[48] B. Perret, K. H. Pawlowski, B. Schartel, *J. Therm. Anal. Calorim.* **2009**, *97*, 949.

[49] P. Müller, M. Morys, A. Sut, C. Jäger, B. Illerhaus, B. Schartel, *Polym. Degrad. Stab.* **2016**, *130*, 307.

[50] K. H. Pawlowski, B. Schartel, M. A. Fichera, C. Jäger, *Thermochim. Acta* **2010**, *498*, 92.

[51] R. E. Lyon, R. N. Walters, *J Anal. Appl. Pyrolisis* **2004**, *71*, 27.

[52] B. Schartel, A. Weiss, *Fire Mater.* **2010**, *34*, 333.

[53] G. M. Wu, B. Schartel, H. Bahr, M. Kleemeier, D. Yu, A. Hartwig, *Combust. Flame* **2012**, *159*, 3616.

[54] U. Braun, U. Knoll, B. Schartel, T. Hoffmann, D. Pospiech, J. Artner, M. Ciesielski, M. Doring, R. Perez-Gratero, J. K. W. Sandler, V. Altstadt, *Macromol. Chem. Phys.* **2006**, *207*, 1501.

[55] Y.-L. Liu, G.-H. Hsiue, C.-W. Lan, Y.-S. Chiu, *Polym. Degrad. Stab.* **1997**, *56*, 291.

[56] C. S. Wang, C. H. Lin, *J. Appl. Polym. Sci.* **1999**, *74*, 1635.

[57] F. Kempel, B. Schartel, G. T. Linteris, S. I. Stoliarov, R. E. Lyon, R. N. Walters, A. Hofmann, *Combust. Flame* **2012**, *159*, 2974.

[58] G. Camino, S. M. Lomakin, M. Lageard, *Polymer* **2002**, *43*, 2011.

[59] G. Camino, S. M. Lomakin, M. Lazzari, *Polymer* **2001**, *42*, 2395.

[60] B. Schartel, T. R. Hull, *Fire Mater.* **2007**, *31*, 327.

[61] M. Ciesielski, B. Burk, C. Heinzmann, M. Döring, in *Novel Fire Retardant Polymers and Composite Materials* (Ed: D.-Y. Wang), Elsevier, Amsterdam, the Netherlands **2017**, pp. 3–51.

[62] F. G. Mann, E. J. Chaplin, *J. Chem. Soc.* **1937**, jr9370000527, https://doi.org/10.1039/jr9370000527.

[63] T. Ranganathan, B.-C. Ku, J. Zilberman, M. Beaulieu, R. J. Farris, E. B. Coughlin, T. Emrick, *J. Polym. Sci., Part A: Polym. Chem.* **2007**, *45*, 4573.

[64] L. C. Thomas, *Interpretation of the Infrared Spectra of Organophosphorus Compounds*, Heyden, London **1974**.